2024 IEEE International Conference on Robotics and Automation (ICRA 2024)
May 13-17, 2024. Yokohama, Japan

Generation of Steady Wheel Gait for Planar X-shaped Walker with Reaction Wheel

Fumihiko Asano[1], Taiki Sedoguchi[1] and Cong Yan[2]

Abstract— **This paper addresses the problem of realizing a novel robotic bipedal locomotion called wheel gait, which is achieved by rotating the stance and swing legs in the same direction. First, a model of a planar 3-DOF X-shaped walker with a reaction wheel is introduced, and the mathematical equations are described. Second, the condition for stabilizing zero dynamics is formulated as the time integral value of control input to the reaction wheel for one step becomes zero, and the control system for achieving this is designed based on the method of continuous-time output deadbeat control. Third, a typical steady wheel gait of the linearized model is numerically generated, and its extension to the nonlinear model is discussed. Although the nonlinear model has only one nonlinear term in the gravity term, numerical simulations show that there is a big gap between this and the linearized model. Through analysis of the typical nonlinear wheel gaits, the difficulty of achieving the same walking speed as the linearized model is discussed.**

I. INTRODUCTION

In a simple compass-like bipedal robot with two leg frames connected at the active hip joints, the stance and swing legs are always driven in opposite directions by applying the hip-joint torque, so it is possible to walk in the same manner as a human (normal gait). The stance leg rotates forward around the ground-contact point, whereas the swing leg rotates in the opposite direction around the hip joint and overtakes the stance leg. From this, it can be explained that the property that the two leg frames rotate in opposite directions is the most essential feature of bipedal locomotion. When walking using two leg frames of the same length, however, a problem always arises as to how to ensure the clearance of the swing foot with respect to the ground surface. In order to solve this problem, the authors recently started the study on a novel bipedal locomotion called wheel gait, in which the two leg frames rotate in the same direction. This problem was first addressed by Kiefer and Ramesh [1]. They introduced a planar 3-DOF X-shaped walker with a reaction wheel sandwiched between two leg frames, and discussed methods for generating normal and wheel gaits. After that, Spong et al. also investigated methods for generating normal gaits using the same model [2], [3]. In addition to these, several studies have been reported so far regarding legged locomotion robots with a body structure in which a reaction wheel (torso or flywheel) is sandwiched between two leg frames [4]–[7]. In models where the center of mass (COM) of the leg frames is below the hip joint, natural swinging motion of the legs occurs due to the action of gravity, and an efficient gait can be generated on a gentle downhill or a horizontal plane by applying small driving force. A major feature of the X-shaped walker model is, however, that the COM of the leg frames is located at the same position as the hip joint, and natural swinging motion of the legs does not occur. Therefore, as mathematically and experimentally investigated by Asano [8], it cannot generate a stable passive-dynamic gait on a gentle downhill.

The most attractive feature of the wheel gait is that there is no need to care about swing-foot clearance or foot scuffing at midstance. Little research, however, has been conducted to date because it is impossible to generate a stable wheel gait with a body structure consisting only of leg frames, and because it is difficult to stabilize zero dynamics.

The purpose of our study is to clearly formulate the mathematical equations and stability conditions for zero dynamics of a 3-DOF X-shaped walker, and to identify problems in the design of its control system. First, we introduce the X-shaped walker model that consists of two identical leg frames and a reaction wheel sandwiched between them, and develop the mathematical equations of motion and collision. Second, we discuss the necessary condition for stabilizing the reaction wheel motion or zero dynamics, and design a control system for generating a steady wheel gait based on the method of continuous-time output deadbeat control (CODC) [9], [10]. Third, we numerically generate a typical wheel gait of the linearized model, and discuss the problems in extension to the nonlinear model. Through numerical investigations, we show that there is a big gap between the linearized model and nonlinear model, and that the steady step period of the latter becomes more than double that of the former.

II. MODELING

Fig. 1 shows the overview and coordinate system of the robot. This is a 3-DOF model consisting of two identical leg frames and a reaction wheel sandwiched between them. We assume that the stance foot is in contact with the ground at one point without sliding. Here, θ_1 and θ_2 are the absolute angles of the stance and swing legs relative to the vertical up direction, and θ_3 is that of the reaction wheel with respect to the horizontal forward direction. The mass and inertia moment around the COM of the leg frame are m_L and I_L, and those of the reaction wheel are m_R and I_R. These

This research was partially supported by Grant-in-Aid for Scientific Research (C) No. 23K03727, provided by the Japan Society for the Promotion of Science (JSPS).

[1]F. Asano and T. Sedoguchi are with the Graduate School of Advanced Science and Technology, Japan Advanced Institute of Science and Technology, 1-1 Asahidai, Nomi, Ishikawa 923-1292, Japan {fasano,sedoguchi}@jaist.ac.jp

[2]C. Yan is with the Department of Mechanical Engineering, Ritsumeikan University, 1-1-1 Nojihigashi, Kusatsu, Shiga 525-8577, Japan gansou@fc.ritsumei.ac.jp

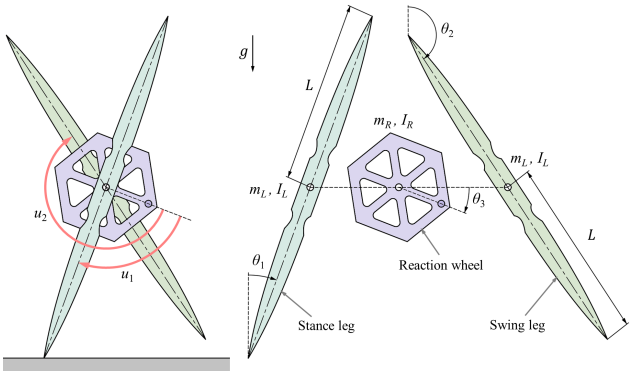

Fig. 1. Model of planar X-shaped walker with reaction wheel

are connected to each other via coaxial active joints, and each COM is located on the axis. L is half the length of the leg frame. The walker can apply a control torque u_1 with a positive clockwise direction from the reaction wheel to the stance leg, and a control torque u_2 from the reaction wheel to the swing leg. Let $\boldsymbol{\theta} = \begin{bmatrix} \theta_1 & \theta_2 & \theta_3 \end{bmatrix}^{\mathrm{T}}$ be the generalized coordinate vector. The robot equation of motion then becomes $\boldsymbol{M}\ddot{\boldsymbol{\theta}} + \boldsymbol{g} = \boldsymbol{S}\boldsymbol{u}$ where

$$\boldsymbol{M} = \begin{bmatrix} mL^2 + I_L & 0 & 0 \\ 0 & I_L & 0 \\ 0 & 0 & I_R \end{bmatrix}, \quad \boldsymbol{g} = \begin{bmatrix} -mgL\sin\theta_1 \\ 0 \\ 0 \end{bmatrix},$$

$$\boldsymbol{S} = \begin{bmatrix} 1 & 0 \\ 0 & 1 \\ -1 & -1 \end{bmatrix}, \quad \boldsymbol{u} = \begin{bmatrix} u_1 \\ u_2 \end{bmatrix},$$

and $m := 2m_L + m_R$ is the robot's total mass.

As described later, the motions of the stance and swing legs are strictly and preferentially controlled to follow their desired time trajectories so that the stance-leg exchange collision can be always performed in the same state and posture according to the method of CODC. In the following, the superscripts "$-$" and "$+$" shall denote immediately before and immediately after impact, and T shall denote the step period defined as the time interval from an instant of stance-leg exchange to the next, which is identical to the target settling time. As illustrated in Fig. 2(a), the walker shall always start motion from the following target state immediately after impact.

$$\begin{bmatrix} \theta_1 \\ \theta_2 \\ \theta_3 \end{bmatrix}^{+} = \begin{bmatrix} \theta_1(0^+) \\ \theta_2(0^+) \\ \theta_3(0^+) \end{bmatrix} = \begin{bmatrix} -\frac{\alpha}{2} \\ \frac{\alpha}{2} \\ \theta_3^* \end{bmatrix} \tag{1}$$

Here, α is half the magnitude of the relative hip-joint angle at impact. By appropriately controlling the motion during the single-limb support phase, the terminal state shown in Fig. 2(e) is always settled to the following state immediately before the next impact.

$$\begin{bmatrix} \theta_1 \\ \theta_2 \\ \theta_3 \end{bmatrix}^{-} = \begin{bmatrix} \theta_1(T^-) \\ \theta_2(T^-) \\ \theta_3(T^-) \end{bmatrix} = \begin{bmatrix} \frac{\alpha}{2} \\ \pi - \frac{\alpha}{2} \\ \theta_3^* \end{bmatrix} \tag{2}$$

After stance-leg exchange, this is reset to Eq. (1) again. The angular positions of the leg frames, θ_1 and θ_2, can be controlled without difficulty, but stabilizing zero dynamics of the reaction wheel is not easy. For simplicity, in this paper we set the target initial and terminal angular positions, $\theta_3^* = \theta_3(0^+) = \theta_3(T^-)$, to zero. The problem in stabilizing zero dynamics is how to determine the target initial angular velocity as described later.

We assume that the rear foot takes off immediately after the fore foot makes a completely inelastic collision with the ground. The X-shaped walker has a special property that the angular velocity of the rear leg does not change at collision, that is, $\dot{\theta}_1^- = \dot{\theta}_2^+$ holds [1] [2] [11]. The angular velocity of the reaction wheel is also not affected by collision, and $\dot{\theta}_3^- = \dot{\theta}_3^+$ holds. Only the angular velocity of the fore leg decreases by collision, and the relationship is specified as $\dot{\theta}_1^+ = \xi\dot{\theta}_2^-$. The transition equation of the angular velocities then becomes

$$\begin{bmatrix} \dot{\theta}_1 \\ \dot{\theta}_2 \\ \dot{\theta}_3 \end{bmatrix}^{+} = \begin{bmatrix} 0 & \xi & 0 \\ 1 & 0 & 0 \\ 0 & 0 & 1 \end{bmatrix} \begin{bmatrix} \dot{\theta}_1 \\ \dot{\theta}_2 \\ \dot{\theta}_3 \end{bmatrix}^{-}, \tag{3}$$

where

$$\xi = \frac{mL^2\cos\alpha + I_L}{mL^2 + I_L}, \tag{4}$$

and this is a positive constant less than 1. As described in the next section, in this paper, we design the motion control system so that the angular velocities of the stance and swing legs reach the same terminal value $\dot{\theta}_1^*$ immediately before the next impact, that is, $\dot{\theta}_1(T^-) = \dot{\theta}_2(T^-) = \dot{\theta}_1^*$ is achieved. The angular velocity of the reaction wheel is also controlled to achieve $\dot{\theta}_3(0^+) = \dot{\theta}_3(T^-) = \dot{\theta}_3^*$ by appropriately setting the control parameters. The target steady initial state then becomes

$$\begin{bmatrix} \dot{\theta}_1 \\ \dot{\theta}_2 \\ \dot{\theta}_3 \end{bmatrix}^{+} = \begin{bmatrix} \dot{\theta}_1(0^+) \\ \dot{\theta}_2(0^+) \\ \dot{\theta}_3(0^+) \end{bmatrix} = \begin{bmatrix} 0 & \xi & 0 \\ 1 & 0 & 0 \\ 0 & 0 & 1 \end{bmatrix} \begin{bmatrix} \dot{\theta}_1^* \\ \dot{\theta}_1^* \\ \dot{\theta}_3^* \end{bmatrix} = \begin{bmatrix} \xi\dot{\theta}_1^* \\ \dot{\theta}_1^* \\ \dot{\theta}_3^* \end{bmatrix}. \tag{5}$$

III. CONTROL SYSTEM DESIGN

A. Input-output Linearization for Generating Leg Motions

In the robot equation of motion described above, the equations of the stance-leg, the swing leg, and the reaction wheel are respectively specified as

$$\left(mL^2 + I_L\right)\ddot{\theta}_1 - mgL\sin\theta_1 = u_1, \tag{6}$$

$$I_L\ddot{\theta}_2 = u_2, \tag{7}$$

$$I_R\ddot{\theta}_3 = -u_1 - u_2. \tag{8}$$

Since the motions of θ_1 and θ_2 are decoupled, we can consider input-output linearization for them independently. The control input u_1 for achieving $\ddot{\theta}_1 = v_1$ can be determined as

$$u_1 = \left(mL^2 + I_L\right)v_1 - mgL\sin\theta_1, \tag{9}$$

whereas the control input u_2 for achieving $\ddot{\theta}_2 = v_2$ can be determined as

$$u_2 = I_L v_2. \tag{10}$$

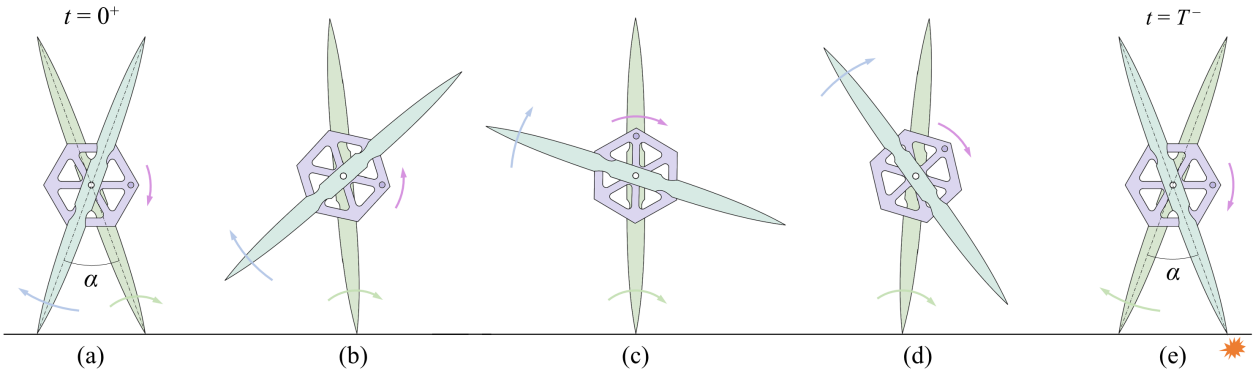

Fig. 2. Motion sequence in wheel gait

The state-space realization for $\ddot{\theta}_j = v_j \ \ (j \in \{1, 2\})$ becomes

$$\frac{\mathrm{d}}{\mathrm{d}t}\begin{bmatrix}\theta_j \\ \dot{\theta}_j\end{bmatrix} = \begin{bmatrix}0 & 1 \\ 0 & 0\end{bmatrix}\begin{bmatrix}\theta_j \\ \dot{\theta}_j\end{bmatrix} + \begin{bmatrix}0 \\ 1\end{bmatrix} v_j. \tag{11}$$

Hereinafter, we denote Eq. (11) as $\dot{\boldsymbol{x}}_j = \boldsymbol{A}\boldsymbol{x}_j + \boldsymbol{B}v_j$. The analytical solution of $\boldsymbol{x}_j$ at t can be solved as

$$\boldsymbol{x}_j(t) = \mathrm{e}^{\boldsymbol{A}t}\boldsymbol{x}_j\left(0^+\right) + \int_{0^+}^{t} \mathrm{e}^{\boldsymbol{A}(t-\tau)}\boldsymbol{B}v_j(\tau)\mathrm{d}\tau. \tag{12}$$

B. Stability Condition of Zero Dynamics

As previously described, the angular positions of the leg frames, θ_1 and θ_2, are preferentially controlled to generate a steady wheel gait. Instead, the reaction wheel behaves as zero dynamics, and the stability is guaranteed by controlling the time integral of the control input to zero as described in the following. The time integral of Eq. (8) becomes

$$\begin{aligned}\int_{0^+}^{T^-} I_R\ddot{\theta}_3 \,\mathrm{d}\tau &= I_R\left(\dot{\theta}_3\left(T^-\right) - \dot{\theta}_3\left(0^+\right)\right) \\ &= -\int_{0^+}^{T^-} \left(u_1(\tau) + u_2(\tau)\right)\mathrm{d}\tau,\end{aligned} \tag{13}$$

and the condition necessary for stabilizing zero dynamics of the reaction wheel is found to be $\dot{\theta}_3\left(T^-\right) = \dot{\theta}_3\left(0^+\right)$. This is equivalent to the condition $J_1 + J_2 = 0$ where

$$J_1 := \int_{0^+}^{T^-} u_1(\tau)\mathrm{d}\tau, \quad J_2 := \int_{0^+}^{T^-} u_2(\tau)\mathrm{d}\tau. \tag{14}$$

The angular position immediately before the next impact can be solved as

$$\begin{aligned}\theta_3\left(T^-\right) &= \theta_3\left(0^+\right) + \dot{\theta}_3\left(0^+\right)T \\ &\quad + \int_{0^+}^{T^-} \frac{\left(u_1(\tau) + u_2(\tau)\right)\left(\tau - T\right)}{I_R}\mathrm{d}\tau.\end{aligned} \tag{15}$$

Then, under the conditions of $J_1 + J_2 = 0$ and $\theta_3\left(T^-\right) = \theta_3\left(0^+\right)$, the target angular velocity immediately after impact can be solved as

$$\dot{\theta}_3\left(0^+\right) = -\int_{0^+}^{T^-} \frac{\left(u_1(\tau) + u_2(\tau)\right)\tau}{I_R T}\mathrm{d}\tau. \tag{16}$$

An approximate analytical solution for $\dot{\theta}_3^* := \dot{\theta}_3\left(T^-\right) = \dot{\theta}_3\left(0^+\right)$ can be obtained using a linearized model. The solution to the nonlinear model, however, can only be obtained by conducting numerical integration for one step.

C. Design of CODC for Swing-leg Motion

The angular position and angular velocity of the swing leg immediately after impact are always $\theta_2\left(0^+\right) = \frac{\alpha}{2}$ and $\dot{\theta}_2\left(0^+\right) = \dot{\theta}_1^*$, and those immediately before the next impact to be achieved are $\theta_2\left(T^-\right) = \pi - \frac{\alpha}{2}$ and $\dot{\theta}_2\left(T^-\right) = \dot{\theta}_1^*$. As the easiest way to smoothly interpolate these states, we consider a CODC system in the following.

The time integral of the swing-leg motion for one step becomes

$$\int_{0^+}^{T^-} I_L\ddot{\theta}_2 \,\mathrm{d}\tau = I_L\left(\dot{\theta}_2\left(T^-\right) - \dot{\theta}_2\left(0^+\right)\right) = \int_{0^+}^{T^-} u_2(\tau)\mathrm{d}\tau. \tag{17}$$

The condition necessary for $\dot{\theta}_2\left(T^-\right) = \dot{\theta}_2\left(0^+\right)$ is therefore equivalent to $J_2 = 0$. In the target swing-leg motion to be realized, however, $\dot{\theta}_2\left(T^-\right) = \dot{\theta}_2\left(0^+\right) = \dot{\theta}_1^*$ holds. Therefore, $J_2 = 0$ also holds automatically, and the target terminal conditions to be met are finally found to be two; the condition for the angular position and that for the angular velocity mentioned above. It is then sufficient to consider v_2 as a linear time function with two undetermined coefficients, that is, $v_2(t) = \beta_1 t + \beta_0 =: \ddot{\theta}_{2\mathrm{d}}(t)$. By substituting this into Eq. (7) and solving the terminal state, the target condition can be obtained as

$$\begin{aligned}\boldsymbol{x}_2\left(T^-\right) &= \mathrm{e}^{\boldsymbol{A}T}\boldsymbol{x}_2\left(0^+\right) + \int_{0^+}^{T^-} \mathrm{e}^{\boldsymbol{A}(T-\tau)}\boldsymbol{B}v_2(\tau)\mathrm{d}\tau \\ &= \begin{bmatrix}\frac{\alpha}{2} + \frac{\beta_1 T^3}{6} + \frac{\beta_0 T^2}{2} + \dot{\theta}_1^* T \\ \frac{\beta_1 T^2}{2} + \beta_0 T + \dot{\theta}_1^*\end{bmatrix} = \begin{bmatrix}\pi - \frac{\alpha}{2} \\ \dot{\theta}_1^*\end{bmatrix}.\end{aligned} \tag{18}$$

By solving Eq. (18) for β_1 and β_0, we obtain

$$\beta_1 = \frac{12}{T^3}\left(\dot{\theta}_1^* T + \alpha - \pi\right), \tag{19}$$

$$\beta_0 = -\frac{6}{T^2}\left(\dot{\theta}_1^* T + \alpha - \pi\right). \tag{20}$$

D. Design of CODC for Stance-leg Motion

The angular position and angular velocity of the stance leg immediately after impact are always $\theta_1\left(0^+\right) = -\frac{\alpha}{2}$ and $\dot{\theta}_1\left(0^+\right) = \xi\dot{\theta}_1^*$, and those immediately before the next impact to be achieved are $\theta_1\left(T^-\right) = \frac{\alpha}{2}$ and $\dot{\theta}_1\left(T^-\right) = \dot{\theta}_1^*$. To smoothly interpolate these states, we consider a CODC system again.

As described in the previous subsection, the condition $J_2 = 0$ has already been achieved, and the target conditions to be met are now found to be three; the condition for the terminal angular position, that for the terminal angular velocity, and $J_1 = 0$. It is then sufficient to consider v_1 as a second-order time function with three undetermined coefficients, that is, $v_1(t) = \gamma_2 t^2 + \gamma_1 t + \gamma_0 =: \ddot{\theta}_{1\mathrm{d}}(t)$. By substituting this into Eq. (6) and solving the terminal state, the target condition can be obtained as

$$\begin{aligned}\boldsymbol{x}_1\left(T^-\right) &= \mathrm{e}^{\boldsymbol{A}T}\boldsymbol{x}_1\left(0^+\right) + \int_{0^+}^{T^-} \mathrm{e}^{\boldsymbol{A}(T-\tau)}\boldsymbol{B}v_1(\tau)\mathrm{d}\tau \\ &= \begin{bmatrix} -\frac{\alpha}{2} + \frac{\gamma_2 T^4}{12} + \frac{\gamma_1 T^3}{6} + \frac{\gamma_0 T^2}{2} + \xi\dot{\theta}_1^* T \\ \frac{\gamma_2 T^3}{3} + \frac{\gamma_1 T^2}{2} + \gamma_0 T + \xi\dot{\theta}_1^* \end{bmatrix} \\ &= \begin{bmatrix} \frac{\alpha}{2} \\ \dot{\theta}_1^* \end{bmatrix}. \end{aligned} \tag{21}$$

On the other hand, by considering the following linear approximation in Eq. (9):

$$\sin\theta_1(t) \approx \theta_1(t) = -\frac{\alpha}{2} + \frac{\gamma_2 t^4}{12} + \frac{\gamma_1 t^3}{6} + \frac{\gamma_0 t^2}{2} + \xi\dot{\theta}_1^* t, \tag{22}$$

the approximate analytical solution and target condition for J_1 can be obtained as

$$\begin{aligned} J_1 \approx& \int_{0^+}^{T^-} \left(\left(mL^2 + I_L\right)v_1(\tau) - mgL\theta_1(\tau)\right)\mathrm{d}\tau \\ =& \frac{T}{120}\left(2\left(20(mL^2+I_L) - mgLT^2\right)T^2\gamma_2\right. \\ &+5\left(12(mL^2+I_L) - mgLT^2\right)T\gamma_1 \\ &+20\left(6(mL^2+I_L) - mgLT^2\right)\gamma_0 \\ &\left.+60mgL\left(\alpha - \xi\dot{\theta}_1^* T\right)\right) = 0. \end{aligned} \tag{23}$$

By solving Eqs. (21) and (23) for the coefficients, we obtain

$$\gamma_2 = \frac{30\dot{\theta}_1^*}{mgLT^5}\left(12\left(mL^2+I_L\right) + mgLT^2\right)(1-\xi), \tag{24}$$

$$\begin{aligned}\gamma_1 = -\frac{12}{mgLT^4}&\left(30\dot{\theta}_1^*\left(mL^2+I_L\right)(1-\xi) + mgLT\alpha\right. \\ &\left.+mgLT^2\dot{\theta}_1^*(2-3\xi)\right), \end{aligned} \tag{25}$$

$$\begin{aligned}\gamma_0 = \frac{1}{mgLT^3}&\left(60\dot{\theta}_1^*\left(mL^2+I_L\right)(1-\xi) + 6mgLT\alpha\right. \\ &\left.+3mgLT^2\dot{\theta}_1^*(1-3\xi)\right). \end{aligned} \tag{26}$$

With these coefficients, the stance-leg angle is controlled to follow the trajectory of Eq. (22) and satisfies the target boundary conditions according to the method of CODC. Note that, however, since a linear approximation is used for the condition $J_1 = 0$, this is not satisfied in the nonlinear model.

IV. WHEEL GAIT GENERATION

A. Typical Steady Wheel Gait of Linearized Model

In this section, we first generate a steady wheel gait of the linearized model, and based on the results, we attempt to extend it to the nonlinear model. In the robot equation of motion, the only nonlinear term is $-mgL\sin\theta_1$ in Eq. (6), and the linearized model can be obtained only by approximating it to $-mgL\theta_1$. By using the linear approximation of Eq. (22) again, an approximate analytical solution of the target initial angular velocity of the reaction wheel can be derived by Eq. (16) as

$$\begin{aligned}\dot{\theta}_3^* = &-\frac{\dot{\theta}_1^*\left(mL\left(60L + gT^2\right)(1+\xi) + 60I_L(3+\xi)\right)}{120I_R} \\ &+\frac{I_L\pi}{I_R T} + \frac{mL\alpha\left(10L + gT^2\right)}{10I_R T}. \end{aligned} \tag{27}$$

First, we tried to generate a steady wheel gait of the linearized model by setting $v_j(t)$ only to the angular acceleration command signal, $\ddot{\theta}_{j\mathrm{d}}(t)$, mentioned above. As a result, however, we confirmed that the walking motion could be generated for a few steps according to the method, but it gradually diverged. This was due to the integration of small numerical errors that occurred during collisions. We then added PD feedback control terms to $v_j(t)$ as

$$v_j(t) = \ddot{\theta}_{j\mathrm{d}}(t) + K_D\left(\dot{\theta}_{j\mathrm{d}}(t) - \dot{\theta}_j\right) + K_P\left(\theta_{j\mathrm{d}}(t) - \theta_j\right), \tag{28}$$

where K_D and K_P are the derivative and proportional gains.

Fig. 3 shows the simulation results of steady wheel gait generation of the linearized model with PD feedback control. The physical and control parameters where chosen as the values listed in Table I. We can see that a steady wheel gait has been successfully generated. From Fig. 3(c), we can see that both u_1 and u_2 take positive values in the first half of the cycle, but decrease to negative values in the second half,

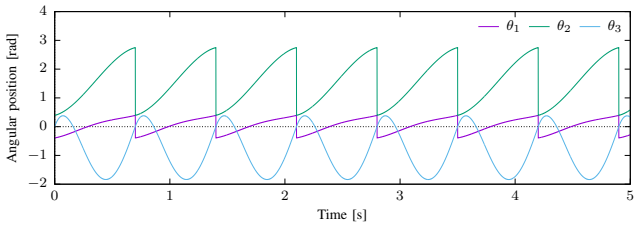

(a) Angular position

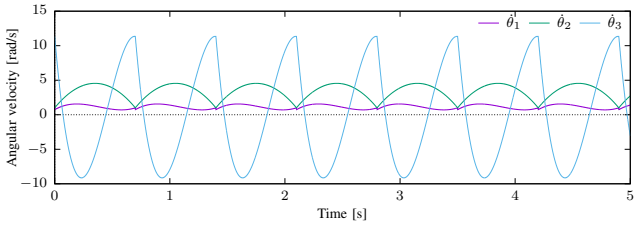

(b) Angular velocity

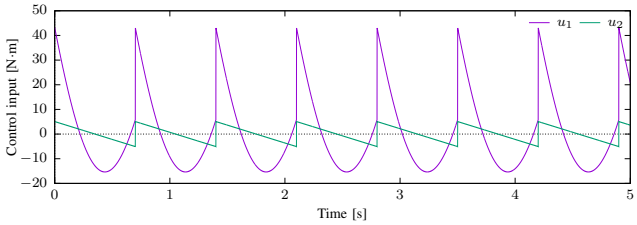

(c) Control input

Fig. 3. Simulation results of steady wheel gait of linearized model

TABLE I

PHYSICAL AND CONTROL PARAMETERS

m_L	1.0	kg
m_R	1.0	kg
I_L	0.25	kg·m^2
I_R	0.25	kg·m^2
L	1.0	m
T	0.7	s
α	$\frac{\pi}{4}$	rad
ξ	0.729637	-

$\dot{\theta}_1^*$	1.0	rad/s
$\dot{\theta}_3^*$	11.3499	rad/s
β_1	-57.9427	rad/s^3
β_0	20.2799	rad/s^2
γ_2	87.5987	rad/s^4
γ_1	-67.6173	rad/s^3
γ_0	9.74452	rad/s^2
K_D	100	s^{-1}
K_P	2500	s^{-2}

and the time integral values for one step become zero. From Figs. 3(a) and (b), we can see that the stance leg, swing leg and reaction wheel generated a steady motion.

Fig. 4 shows the phase-plane plot of the generated motions of the reaction wheel without and with PD feedback control. We can see that there is a big difference in the stability of the generated motion depending on whether PD feedback control is applied or not.

B. Extension to Nonlinear Model

Based on the results of the linearized model, now we discuss steady wheel gait generation for the nonlinear model. Regardless of whether the model is linearized or nonlinear, the condition $J_2 = 0$ is always achieved, so the problem is how to achieve $J_1 = 0$ in the nonlinear model. As suggested by $\boldsymbol{x}_1(T^-)$ in Eq. (21), the stance-leg motion is regulated by two parameters T and $\dot{\theta}_1^*$. Therefore, we initially expected that the condition $J_1 = 0$ could be achieved by adjusting the two parameters in the nonlinear model as well. In reality, however, as described below, there is a big gap between the linearized model and the nonlinear model, and it has been clarified that the steady step period of the latter is significantly different from the former.

Fig. 5 shows the analysis results of (a) J_1 with respect to

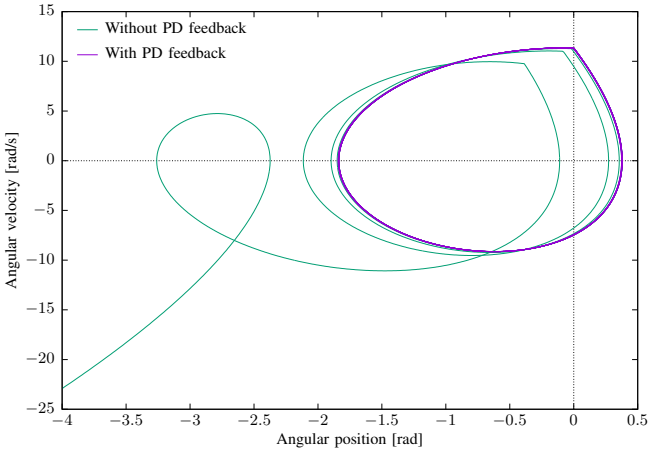

Fig. 4. Phase-plane plot of generated motions of reaction wheel without and with PD feedback control

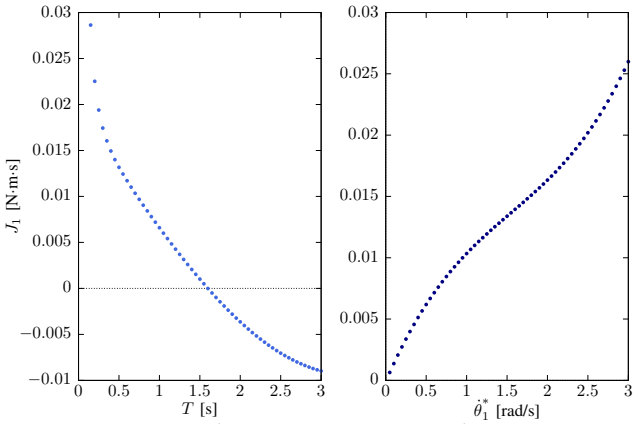

(a) J_1 vs T where $\dot{\theta}_1^* = 1.0$ [rad/s] (b) J_1 vs $\dot{\theta}_1^*$ where $T = 0.7$ [s]

Fig. 5. J_1 versus system parameters in nonlinear model

T where $\dot{\theta}_1^* = 1.0$ [rad/s], and (b) that with respect to $\dot{\theta}_1^*$ where $T = 0.7$ [s]. As seen in (a), there is a solution of T that achieves $J_1 = 0$. In (b), however, it can be seen that J_1 is always positive and there is no solution of $\dot{\theta}_1^*$ that achieves $J_1 = 0$. Based on this fact, in the following we consider T as the only control parameter and investigate its effect on the nonlinear wheel gait.

First, we numerically generate the steady wheel gait of the nonlinear model with the target T in Fig. 5(a). The value achieving $J_1 = 0$ was identified as $T = 1.5993$ [s]. The target initial/terminal angular velocity of the reaction wheel was also numerically identified as $\dot{\theta}_3^* = 5.92375$ [rad/s] by Eq. (16). Since there is a big gap between the values of T and $\dot{\theta}_3^*$ obtained numerically and those in Table I, generating a steady nonlinear wheel gait is possible, but the generated one would be significantly different from that of the linearized model. Fig. 6 shows the simulation results of steady wheel gait generation of the nonlinear model with PD feedback control. The system parameters except T and $\dot{\theta}_3^*$ were chosen as the values listed in Table I again. As expected, a very slow motion with a step period more than twice that of the linearized model has been generated.

Fig. 7 shows the analysis result of J_1 with respect to T for six values of $\dot{\theta}_1^*$. We can see that when the value of $\dot{\theta}_1^*$ is 0.5 or 1.0 [rad/s], J_1 decreases monotonically with increase of T, but when the value of $\dot{\theta}_1^*$ becomes 1.5 or more, J_1 decreases once, reaches a minimum value, and then begins to increase again. Among them, when $\dot{\theta}_1^* = 2.0$ [rad/s], there are two solutions for T that achieve $J_1 = 0$; the values were numerically identified as $T = 1.38566$ and 2.06523 [s]. Hereinafter, the steady wheel gait with the shorter settling time is referred to as short-period gait, and that with the longer one is referred to as long-period gait. Fig. 8 shows the phase-plane plot of the generated stance-leg motions in the short- and long-period gaits where $\dot{\theta}_1^* = 2.0$ [rad/s]. In each case, we can see that according to the method, the stance-leg motion starts from the target initial state and reaches the target terminal state, but that the motion exhibits a complex movement in which the rotational motion is reversed at mid-stance. As the initial angular velocity setting increases, it

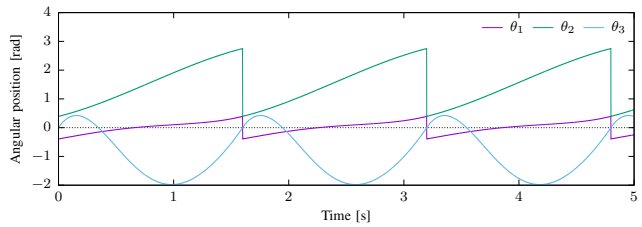

(a) Angular position

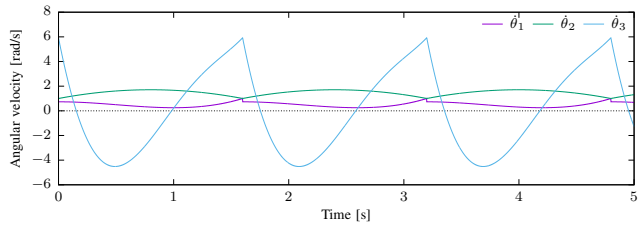

(b) Angular velocity

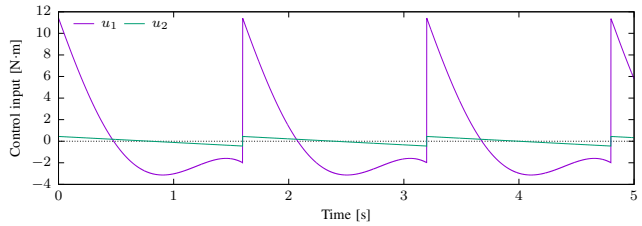

(c) Control input

Fig. 6. Simulation results of steady wheel gait of nonlinear model

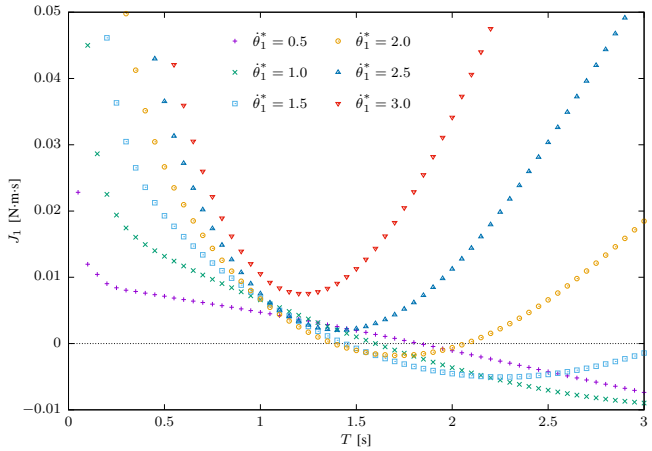

Fig. 7. J_1 with respect to T for six values of $\dot{\theta}_1^*$

tends to be difficult to generate a smooth wheel gait as shown in Fig. 8. This is probably because the initial angular velocity $\dot{\theta}_1^*$ became too large compared to the target settling time, and it became necessary to ensure time by braking the stance-leg motion.

C. Discussion

In legged locomotion that does not include state jumps caused by collisions for stance-leg exchange, such as collisionless or stealth walking [12]–[15], spatio-temporal (time-reversal) symmetry in the trajectories of the leg motions and control inputs are achieved on the phase plane. In limit cycle walking that includes collisions, however, the

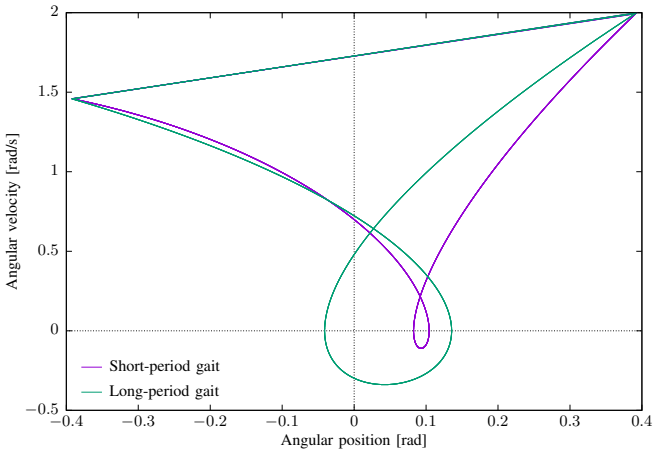

Fig. 8. Phase-plane plot of generated steady stance-leg motions in short- and long-period gaits where $\dot{\theta}_1^* = 2.0$ [rad/s]

spatio-temporal symmetry of those is disrupted, resulting in complex problems such as the big gap described above.

In this paper, we designed the leg motions based on the method of CODC with minimal unknown coefficients, but it is also necessary to consider other approaches that do not create the big gap. Since the control input u_1 includes a nonlinear term $\sin\theta_1$, and its time integral produces the gap, we should consider another approach in which the angular acceleration command signal, $v_1(t) = \ddot{\theta}_{1\mathrm{d}}(t)$, can be specified as a lower-order function of time.

The energy efficiency of the generated gait can be evaluated using specific resistance (SR) [9], [14], which represents the amount of energy consumed to move a unit mass a unit distance. The values of SR in the linearized gait of Fig. 3 and the nonlinear gait of Fig. 6 were 2.63507 and 0.604663 [-], respectively. This means that the latter is significantly more energy efficient, and that there is a trade-off between the walking speed and energy efficiency. Although it is difficult to achieve high-speed walking with the nonlinear model, the control input load is greatly reduced, resulting in highly efficient movement.

V. CONCLUSION AND FUTURE WORK

In this paper, we investigated the method for generating a steady wheel gait of the planar X-shaped walker with a reaction wheel, and numerically showed that the nonlinear model can generate a steady wheel gait but the resultant step period of it was found to be very long and significantly different from that of the linearized model. In order to eliminate this gap and generate a high-speed nonlinear wheel gait, we should investigate methods of generating stance-leg motion other than CODC in the future.

Although we limited our discussion to the problem of generating a steady wheel gait in this paper, it is also necessary to consider asymptotically stable wheel gaits with more relaxed boundary conditions. Furthermore, we should investigate extension to the problems of climbing stairs and walking on uneven terrain by making full use of the features of the wheel gait.

REFERENCES

[1] J. Kiefer and B. Ramesh, "Walking viability and gait synthesis for a novel class of dynamically-simple bipeds." *Informatica*, Vol. 17, Iss. 2, pp. 145–155, 1993.

[2] M. W. Spong, R. Lozano and R. Mahony, "An almost linear biped," *Proc. of the 39th IEEE Conf. on Decision and Control*, pp. 4803–4808, 2000.

[3] T. G. McGee and M. W. Spong, "Trajectory planning and control of a novel walking biped," *Proc. of the IEEE Int. Conf. on Control Applications*, pp. 1099–1104, 2001.

[4] P. Rouchon and H. Sira-Ramirez, "Control of the walking toy: a flatness approach," *Proc. of the American Control Conference*, pp. 2018–2023, 2003.

[5] T. Kinugasa, Y. Hashimoto and H. Fushimi, "Passive walking of biped emu with attitude control of body," *Proc. of the IEEE/RSJ Int. Conf. on Intelligent Robots and Systems*, pp. 346–351, 2003.

[6] M. Alba, J. C. G. Prada, J. Meneses and H. Rubio, "Center of percussion and gait design of biped robots," *Mechanism and Machine Theory*, Vol. 45, Iss. 11, pp. 1681–1693, 2010.

[7] C. E. de Brito Novaes, P. S. P. da Silva and P. Rouchon, "Trajectory control of a bipedal walking robot with inertial disc," *Proc. of the 19th World Congress*, Vol. 47, Iss. 3, pp. 4843–4848, 2014.

[8] F. Asano, "Simulation and experimental studies on passive-dynamic walker that consists of two identical crossed frames," *Proc. of the IEEE Int. Conf. on Robotics and Automation*, pp. 1703–1708, 2010.

[9] F. Asano, Y. Zheng and X. Xiao, "Time-scale control approaches to collisionless walking of an underactuated rimless wheel," *J. of Robotics and Mechatronics*, Vol. 29, Iss. 3, pp. 471–479, 2017.

[10] F. Asano and X. Xiao, "Output deadbeat control approaches to fast convergent gait generation of underactuated spoked walker," *Proc. of the IEEE/SICE Int. Symp. on System Integration*, pp. 265–270, 2012.

[11] F. Asano and C. Yan, "Low-speed limit cycle walking of planar X-shaped bipedal robot with special properties," *Proc. of the 8th IEEE Int. Conf. on Advanced Robotics and Mechatronics*, pp. 43–48, 2023.

[12] M. W. Gomes and A. Ruina, "Walking model with no energy cost," *Physical Review E*, Vol. 83, Iss. 3, 032901, 2011.

[13] T. Chyou, G. F. Liddell and M. G. Paulin, "An upper-body can improve the stability and efficiency of passive dynamic walking," *J. of Theoretical Biology*, Vol. 285, Iss. 1, pp. 126–135, 2011.

[14] F. Asano and Y. Zheng, "High-speed and energy-efficient collisionless walking of underactuated rimless wheel," *Artificial Life and Robotics*, Vol. 23, Iss. 4, pp. 523–531, 2018.

[15] F. Asano, "Stealth walking with reduced double-limb support phase and its extension to careful legged locomotion," *Multibody System Dynamics*, Vol. 44, Iss. 4, pp. 421–447, 2018.